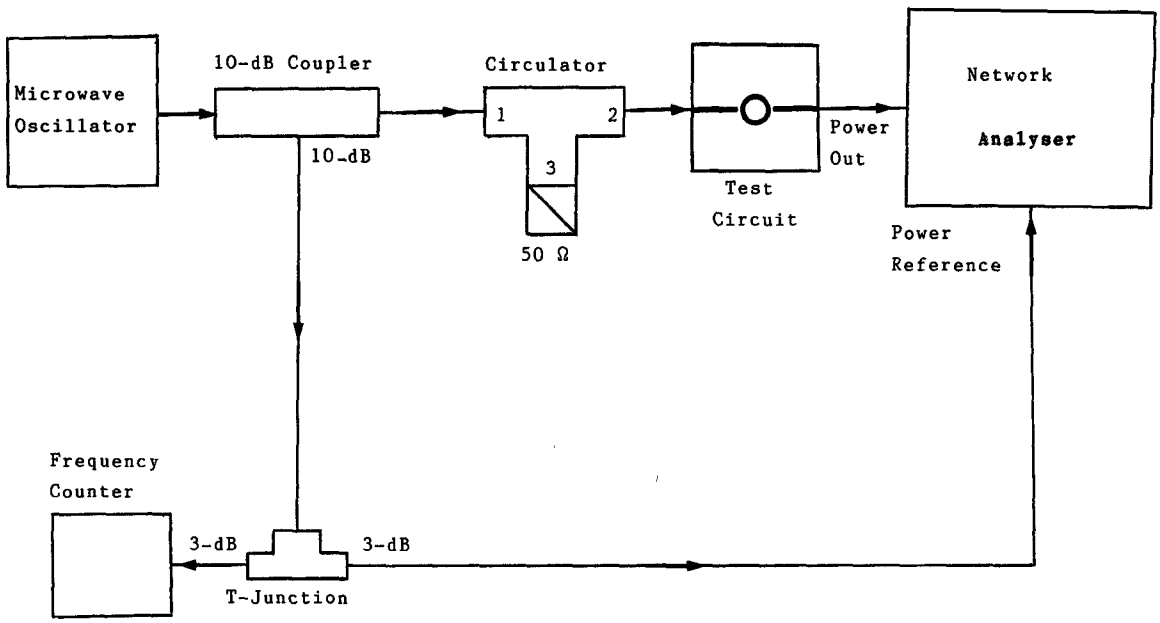

Fig. 5. Resonant frequency measurement setup.

TABLE I

Test Material	ϵ_R	ϵ_C
A	4.0	3.9
	4.0	3.8
	4.2	3.9
B	8.0	9.0
	8.5	9.3
C	2.3	2.2
	2.2	2.3
D	2.8	2.6
	3.2	3.0
	2.8	3.2
E	2.9	2.5
	2.7	2.5
F	7.8	9.3

All measurements were made at 11.5 GHz (unloaded resonant frequency).

frequency drift is a constant and the proportionality rule given by (18) is no longer respected.

Compared with other, more time consuming measurement methods, this method makes it possible to save time and is well suited to material characterization for industrial applications.

References

[1] S. Mao, S. Jones, and G. D. Vendelin, "Millimeter-wave integrated circuits," *IEEE Trans. Microwave Theory Tech.*, vol. MTT-16, pp. 455–461, July 1968.

[2] G. D'inzeo, F. Giannini, C. M. Sodi, and R. Sorrentino, "Method of analysis and filtering properties of microwave planar networks," *IEEE Trans. Microwave Theory Tech.*, vol. MTT-26, pp. 462–471, July 1978.

[3] J. Watkins, "Circular resonant structures in microstrip," *Electron. Lett.*, vol. 5, no. 21, pp. 524–525, Oct. 16, 1969.

[4] T. Itoh and R. Mittra, "A new method for calculating the capacitance of a circular disk for microwave integrated circuits," *IEEE Trans. Microwave Theory Tech.*, vol. MTT-21, pp. 431–432, June 1973.

[5] P. Troughton, "Measurement techniques in microstrip," *Electron. Lett.*, vol. 5, no. 2, pp. 25–26, Jan. 23, 1969.

[6] E. Yamashita and R. Mittra, "Variational method for the analysis of microstrip lines," *IEEE Trans. Microwave Theory Tech.*, vol. MTT-16, pp. 251–256, Apr. 1968.

[7] E. Yamashita, "Variational method for the analysis of microstrip-like transmission lines," *IEEE Trans. Microwave Theory Tech.*, vol. MTT-16, pp. 529–535, Aug. 1968.

[8] R. A. Waldron, "Perturbation theory of resonant cavities," Inst. Electric Engineers, Monograph no. 373E, Apr. 1960.

[9] R. P. Owens, "Accurate analytical determination of quasi-static microstrip line parameters," *Radio Electron. Eng.*, vol. 46, no. 7, pp. 360–364, July 1976.

[10] T. C. Edwards and R. P. Owens, "2–18 GHz dispersions measurements on 10–100 ohm microstrip lines on sapphire," *IEEE Trans. Microwave Theory Tech.*, vol. MTT-24, pp. 506–513, Aug. 1976.

[11] H. A. Wheeler, "Transmission-line properties of parallel wide strips by a conformal mapping approximation," *IEEE Trans. Microwave Theory Tech.*, vol. MTT-12, pp. 280–289, May 1964.

[12] H. A. Wheeler, "Transmission-line properties of parallel strips separated by a dielectric sheet," *IEEE Trans. Microwave Theory Tech.*, vol. MTT-13, pp. 172–185, Mar. 1965.

[13] J. C. Anderson, *Dielectrics*. London: Chapman and Hall, 1964.

Characterization of Microstrip Open End in the Structure of a Parallel-Coupled Stripline Resonator Filter

Tomoki Uwano

Abstract—**This paper describes an accurate characterization of stripline open end in the parallel-coupled microstrip filter configuration. The method of analysis is based on a two-port resonance technique where the spectral-domain approach is used as a full-wave analysis. Even- and odd-mode edge effects are characterized separately by solving transcendental equations. Calculated results are used for the design of certain filters and the experimental results show excellent filter performances, which validates this method and leads to accurate filter design in practice.**

Manuscript received June 12, 1990; revised October 29, 1990.

The author is with the Image Technology Research Laboratory, Matsushita Electric Industrial Company Ltd., 1006 Oaza-kadoma, Osaka 571, Japan.

IEEE Log Number 9041960.

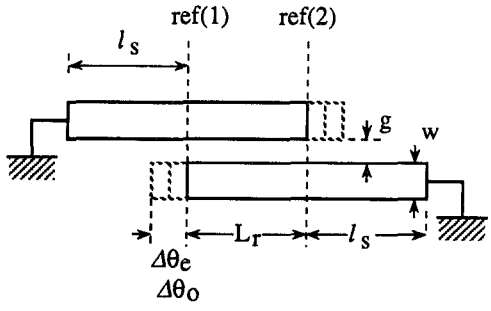

Fig. 1. Circuit configuration of the problem.

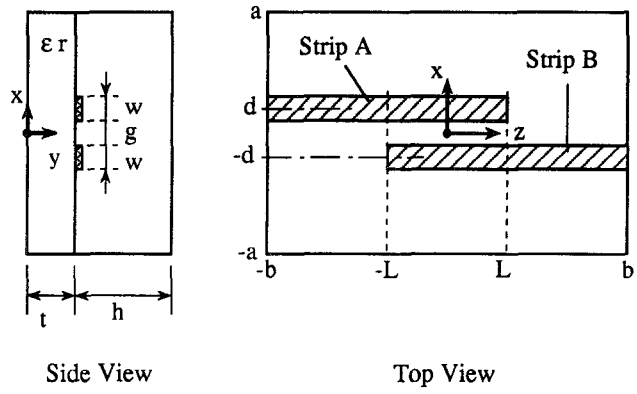

Fig. 2. View of the structure of the problem.

I. Introduction

In a microwave integrated circuit design, a stripline filter is one of the most important circuit elements. Among microstrip filters, the parallel-coupled stripline resonator filter is very popular because of its structural simplicity, and many studies have been carried out on both its theory and design [1]–[3] as well as on structural design formula of even- and odd-mode characteristic impedances for CAD [4]. One problem in this design, however, is dealing with the fringing effect at the open end of each stripline resonator. Because of this discontinuity, the length of a resonator should be slightly shorter than half the wavelength of the propagation. These compensation lengths, usually fixed ones, have been given by a reference table mostly derived from computed or experimental results for the case of a standard stripline resonator. With regard to the characterization of standard stripline open ends including abrupt ends of coupled lines [5], many works by various analysis methods have been reported and several commercial CAD packages are available [6]. As the parallel-coupled striplines have two separate phase velocities, corresponding to the even and odd modes, it is expected that the edge effects in two modes are different from that for the single stripline and vary depending on the stripline gap. Thus, the length of compensation needs adjustment for the variety of designs. Recently, a model including lumped capacitances to account for parasitic coupling and their characterization by computer fitting has been reported [7].

This paper will present the characterization of the edge effects of a parallel-coupled microstrip resonator filter configuration in terms of the equivalent electrical lengths for the even and odd modes respectively in a rigorous manner. The method of analysis is based on a two-port resonance technique [8]. The parallel-coupled stripline section to be analyzed is represented as a two-port network matrix with unknown elements. Then, each port is terminated with a stripline as a known reactance so that the entire structure becomes a resonance circuit.The spectral-domain approach (SDA) [9] is applied to a full-wave analysis, where the resonant frequency is found as an eigenvalue problem.

II. Circuit Representation

The circuit shape of the problem is shown in Fig. 1 along with dimensional parameters. The coupled stripline section is defined between the reference planes, ref(1) and ref(2), and attached by striplines of continuous widths. Thus, the perceived discontinuity is the same as that in the filter structure if l_s is long enough to have continuous propagation fields on the lines.

The electrical length, θ, of the coupled lines can be expressed as

$$\theta_e = \Delta\theta_e + \beta_e L_r$$
$$\theta_o = \Delta\theta_o + \beta_o L_r \tag{1}$$

where subscripts e and o refer to even and odd modes, $\Delta\theta$ represents the discontinuities, and β is the propagation constant. The coupled line section is symmetrically in both the x and z directions and is then represented as a matrix $[Z]$ with two unknown elements:

$$[Z] = \begin{bmatrix} Z11 & Z12 \\ Z12 & Z11 \end{bmatrix} \tag{2}$$

where

$$Z11 = -\frac{1}{2} j\left(Z_{0_e} \cot\theta_e + Z_{0_o} \cot\theta_o\right)$$
$$Z12 = -\frac{1}{2} j\left(Z_{0_e} \csc\theta_e - Z_{0_o} \csc\theta_o\right)$$

$Z_{0_{e,o}}$ being the characteristic impedances in even and odd modes. In assuming that there is no loss, we have two unknowns, $\Delta\theta_e$ and $\Delta\theta_o$, in the matrix. If the two ports are reactively terminated with equal short ended striplines of characteristic impedance Z_s as shown in Fig. 1, the resonance condition is shown [8] as

$$(Z11 + Z_s)^2 - Z12^2 = 0 \tag{3}$$

where

$$Z_s = jZ_0 \tan\beta_S l_S$$

where Z_0 is the characteristic impedance and β_s is the propagation constant of the attached striplines. If the same resonant frequency is obtained with two different pairs of l_s and L_r, (3) yields two different transcendental equations in terms of $\Delta\theta_e$ and $\Delta\theta_o$. These equations may be arithmetically solved by a computer.

III. Resonant Frequency Analysis

For the analysis of the resonant frequency, the circuit in Fig. 1 is enclosed with conducting sidewalls and a top cover. Fig. 2 shows a view of the structure of the problem. The resonant frequency is solved by the SDA method where the currents on the strips are expanded as a set of orthogonal basis functions with unknown coefficients c_μ and d_μ as follows:

$$Jz(x,z) = \sum_{\mu}^{Mz} c_\mu Jz_\mu(x,z)$$
$$Jx(x,z) = \sum_{\mu}^{Mx} d_\mu Jx_\mu(x,z). \tag{4}$$

The basis functions are separable in the x and z directional variables, and assuming the rotational symmetry of the electric and magnetic fields with regard to the planes at $x = 0$ and $z = 0$

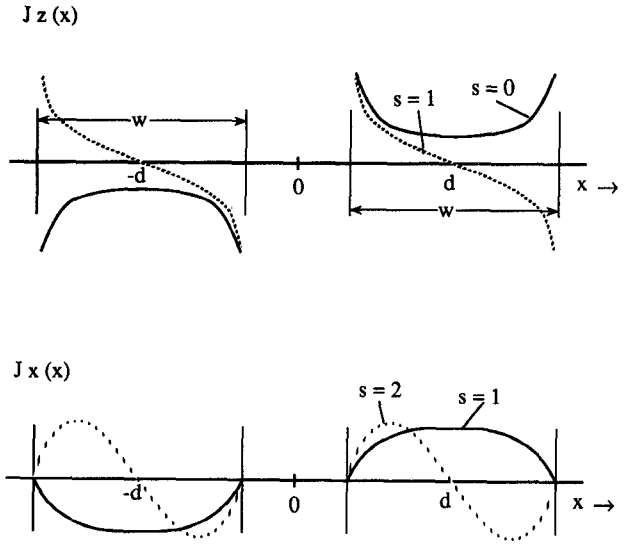

Fig. 3. Shapes of the current basis functions.

respectively, the component functions may be chosen as follows:

$$Jz_r(z) = \cos\frac{2r-1}{2(L+b)}\pi(z \pm b)$$

$$Jx_r(z) = \sin\frac{2r-1}{2(L+b)}\pi(z \pm b)$$

$$Jz_s(x) = \begin{cases} \pm \dfrac{\cos\dfrac{s\pi}{w}(x \mp d)}{\sqrt{1-\left(\dfrac{x \mp d}{w/2}\right)^2}}, & s = 0,2,\cdots \\ -\dfrac{\sin\dfrac{s\pi}{w}(x \mp d)}{\sqrt{1-\left(\dfrac{x \mp d}{w/2}\right)^2}}, & s = 1,3,\cdots \end{cases}$$

$$Jx_s(x) = \begin{cases} \dfrac{\cos\dfrac{s\pi}{w}(x \mp d)}{\sqrt{1-\left(\dfrac{x \mp d}{w/2}\right)^2}}, & s = 1,3\cdots \\ \pm\dfrac{\sin\dfrac{s\pi}{w}(x \mp d)}{\sqrt{1-\left(\dfrac{x \mp d}{w/2}\right)^2}}, & s = 2,4,\cdots \end{cases} \quad (5)$$

Here $\pm$ means that the sign is + on strip A and − on strip B; $\mp$ means that it is − on strip A and + on strip B. The currents are nonzero only on strips A and B. $Jz_s(x)$ being an x-dependent term, it already incorporates the singular behavior of the currents at the stripline edges so that quick convergence is expected. The r and s are to be chosen on the basis of the number μ. Fig. 3 shows the dominant and second-order curves of $Jz(x,0)$ and $Jx(x,0)$ in relation to s.

Fourier transforms of Jz_μ and Jx_μ are then given as

$$\tilde{Jz}_\mu(\alpha,\beta) = \tilde{Jz}_r^A(\beta)\tilde{Jz}_s^A(\alpha) + \tilde{Jz}_r^B(\beta)\tilde{Jz}_s^B(\alpha)$$

$$\tilde{Jx}_\mu(\alpha,\beta) = \tilde{Jx}_r^A(\beta)\tilde{Jx}_s^A(\alpha) + \tilde{Jx}_r^B(\beta)\tilde{Jx}_s^B(\alpha) \quad (6)$$

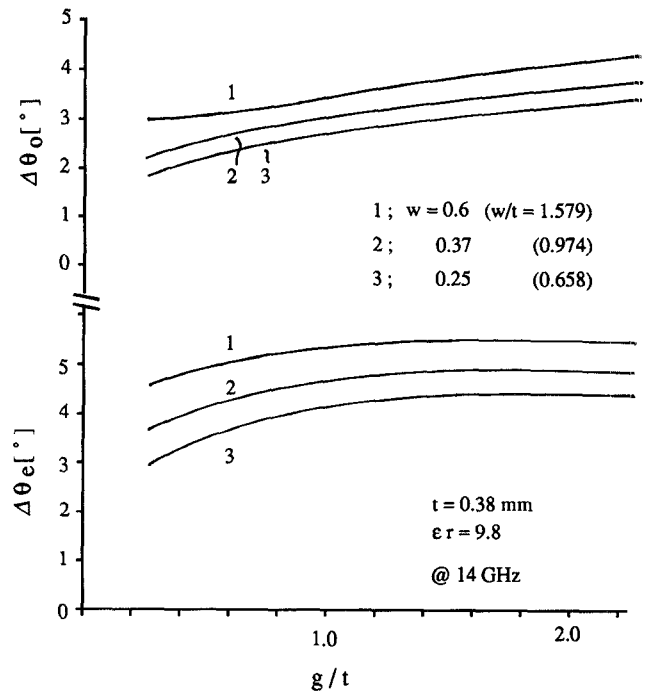

Fig. 4. Calculated results for 0.38-mm-thickness substrate.

where the quantities with the tilde (˜) denote Fourier transforms of corresponding quantities, and the superscripts A and B refer to the components for strips A and B. Each component term in (6) is detailed in the Appendix.

Finally, the homogeneous system of equations is derived with respect to a solution vector $[c_\mu]$ and $[d_\mu]$:

$$\begin{bmatrix} \vdots & \\ \cdots\ e_{ij}\ \cdots & \\ \vdots & \end{bmatrix}\begin{bmatrix} c_\mu \\ \cdots \\ d_\mu \end{bmatrix} = [0]$$

$$e_{ij} = \sum_\alpha \sum_\beta \tilde{Jz}_i \tilde{Z}zz\tilde{Jz}_j \quad \text{for } i \leqslant Mz, \quad j \leqslant Mz$$

$$= \sum\sum \tilde{Jz}_i \tilde{Z}zx\tilde{Jx}_j \quad \text{for } i \leqslant Mz, \quad j \geqslant Mz+1$$

$$= \sum\sum \tilde{Jx}_i \tilde{Z}xz\tilde{Jz}_j \quad \text{for } i \geqslant Mz+1, \quad j \leqslant Mz$$

$$= \sum\sum \tilde{Jx}_i \tilde{Z}xx\tilde{Jx}_j \quad \text{for } i \geqslant Mz+1, \quad j \geqslant Mz+1 \quad (7)$$

where the element e_{ij} is the inner product of the basis functions and Green's function for a single-layer substrate [10]. The matrix is real-symmetric. The condition for a nontrivial solution of (7) is given by the determinant of the matrix equated to zero. This equation may be regarded as a function of ω, L and b:

$$f(\omega, L, b) = 0. \quad (8)$$

For given values of $\omega = \omega_r$, (8) can be solved to evaluate the different pairs of L and b giving rise to the same resonant frequency, ω_r.

IV. Calculated Results

First, the convergence for the solution in (8) was tested in terms of the truncation numbers for α, β, r, and s, and those numbers were chosen in such a way that the convergence error for the final solution in θ is less than 0.2°. Calculated results for the case with $t = 0.38$ mm and $\epsilon_r = 9.8$ at 14 GHz are shown in Fig. 4. The characteristic impedances and phase velocities used

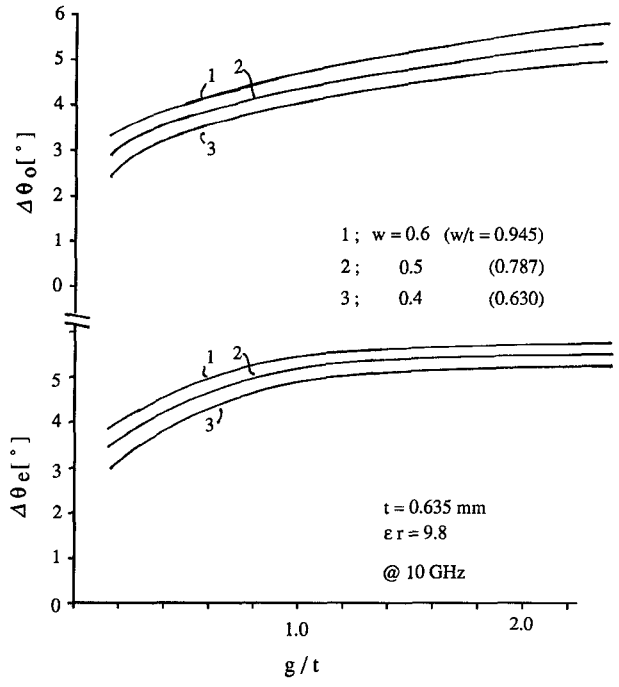

Fig. 5. Calculated results for 0.635-mm-thickness substrate.

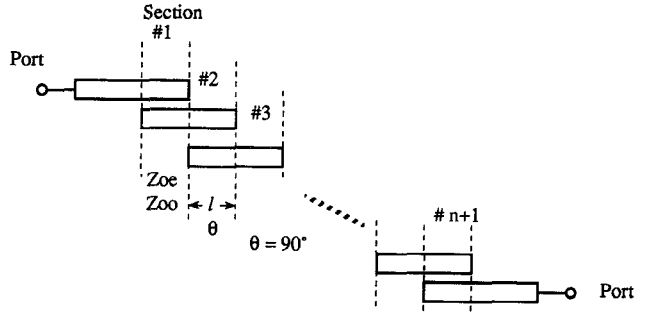

Fig. 6. Parallel-coupled microstrip resonator filter circuit configuration.

TABLE 1
COMPARISON OF THE RESONATOR SECTION LENGTHS

Section No.	l from (9)	l from (10)
1,6	2.033 [mm]	1.967 [mm]
2,5	2.013	1.921
3,4	2.012	1.918

[a]Filter design parameters
Chebyshev response: $n = 5$, $f_0 = 14.25$ GHz, BW = 8%, ripple = 0.1 dB, $t = 0.38$ mm, $2a = 10$ mm, $h = 9$ mm, $\epsilon_r = 9.8$.

in (3) are computed by means of SDA [10] with the same current shapes as shown in Fig. 3. Any spurious solution can be avoided from the insight that $\Delta\theta_e$ should be close to the value for an isolated stripline open end while $\Delta\theta_o$ might have a value between zero and $\Delta\theta_e$ because of the confined fields over the gap and fewer fields at the edge. The uniqueness of the solution was confirmed by examining the different combinations of L and b pairs. The asymptotic values for $\Delta\theta_e$ in Fig. 4 have a perfect match with those estimated from the open end effect of an isolated stripline resonator [11]. The curves for $\Delta\theta_o$ are also expected to reach the same values as a large g in Fig. 4. Another example of calculated results with a substrate thickness of $t = 0.635$ mm at 10 GHz is shown in Fig. 5. Note that for both substrates, the transmission lines propagations already have the dispersion characteristics at those frequencies.

V. Filter Design and Experiments

Design parameters of a parallel-coupled microstrip resonator filter, the configuration of which is shown in Fig. 6, are obtained from a procedure based on the work of Cohn [1]. The length of each section is assumed to be 90° (a quarter wavelength) at the center frequency in the formulation. In the procedure the electrical parameters Z_{0_e} and Z_{0_o} of each section are derived once a frequency response is given. As the phase velocities for even and odd modes are not equal, the physical length, l, of the section which is to be equivalent to a quarter wavelength is expressed as [12]

$$l = \frac{\pi/2}{\bar{\beta} + \dfrac{Z_{0_e} - Z_{0_o}}{Z_{0_e} + Z_{0_o}}\Delta\beta} \tag{9}$$

where

$$\bar{\beta} = \frac{\beta_e + \beta_o}{2} \qquad \Delta\beta = \frac{\beta_e - \beta_o}{2}.$$

By replacing $\beta_e l$ and $\beta_o l$ in (9) with θ_e and θ_o in (1), we obtain a modified form of (9):

$$l = \frac{\dfrac{\pi}{2} - \dfrac{(\Delta\theta_e + \Delta\theta_o)}{2} - \dfrac{Z_{0_e} - Z_{0_o}}{Z_{0_e} + Z_{0_o}}\dfrac{(\Delta\theta_e - \Delta\theta_o)}{2}}{\bar{\beta} + \dfrac{Z_{0_e} - Z_{0_o}}{Z_{0_e} + Z_{0_o}}\Delta\beta}. \tag{10}$$

The second term in the numerator in (10) shows the dominant compensation, which is the average of $\Delta\theta_e$ and $\Delta\theta_o$. The third term may be negligible in comparison with the second term. Table I shows a comparison of the lengths of the sections in one example design case with five resonators. The values used for $\Delta\theta_e$ and $\Delta\theta_o$ are those obtained from Fig. 4. The point Table I suggests is that the structural parameters derived from (9) with or without a uniform length of compensation may cause the untuned frequency condition for some resonators by 0.5 ~ 1.0%. This value is enough to degrade the response curve.

Prior to experiments, the dielectric constant of alumina substrate was accurately estimated to be 9.80 by measurements [11]. Three kinds of experimental filters were designed with a substrate of 0.38 mm thickness using the calculated results in Fig. 4. Fig. 7 shows the experimental results along with the filter design parameters. In this figure, frequency responses of the filters designed from (9) and (10) are illustrated. In a practical design, many designers must have witnessed the same sort of frequency response characteristics as shown in the left in Fig. 7, where the lower half of the passband has a slightly larger insertion loss with the return loss degradation than the rest of the passband. It is intuitively learned that this degradation may be caused by the inaccurate characterization of mainly the first and the last sections, i.e., end resonators, and a prototype filter simulation also has implied the end resonators possibly off-tuned to the higher frequencies. The experimental results with the accurate characterization in Fig. 7 have now verified this. The results exhibit excellent agreement with the prototype responses except for the insertion loss from the resonator unloaded Q. The return loss curves imply well-tuned resonators in the filter. The discrepancy of the center frequencies, about 0.2 ~ 0.7%, is con

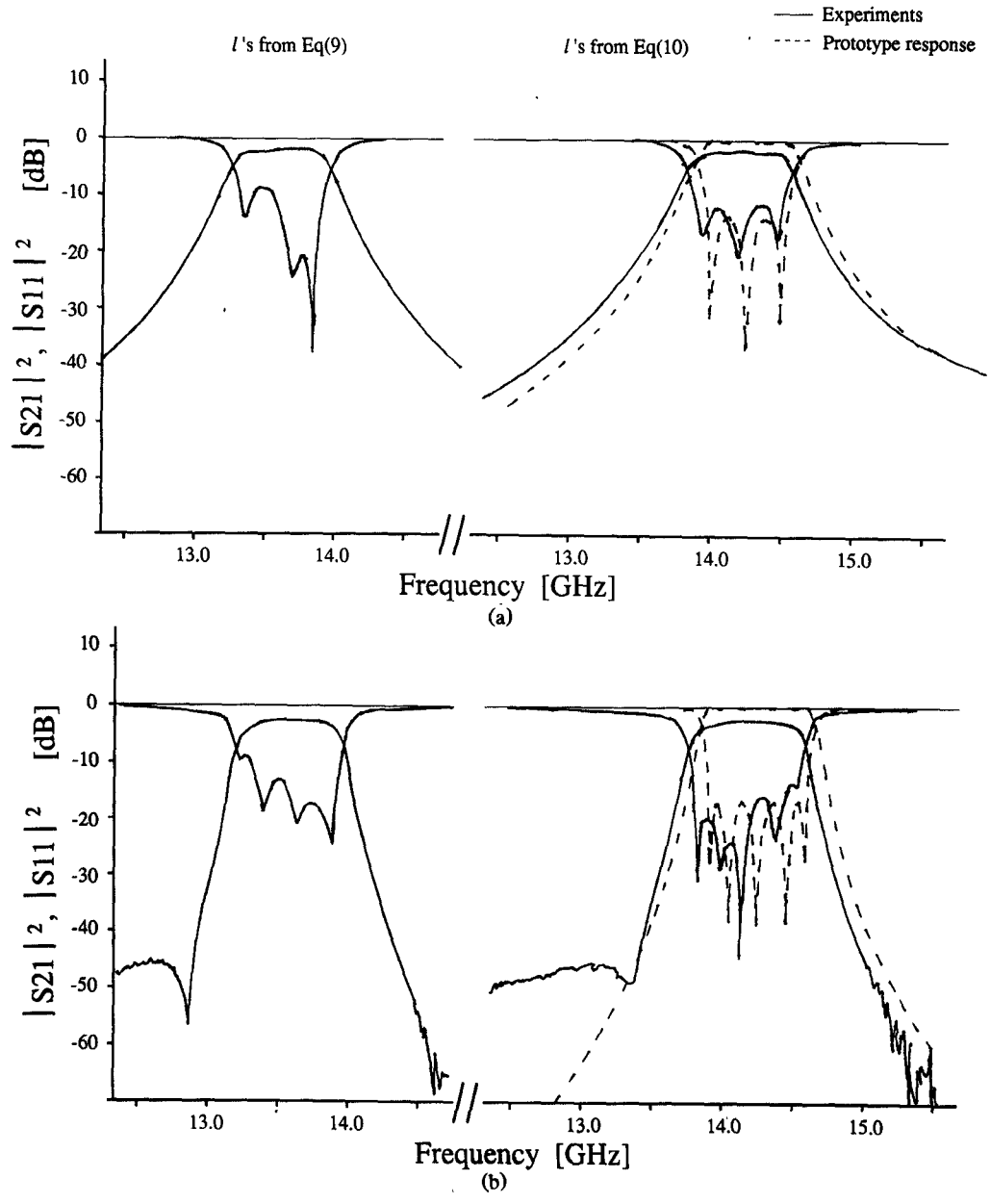

Fig. 7. Experimental results with design parameters of Chebyshev response and (a) $n = 3$, bandwidth = 4%, ripple = 0.2 dB; (b) $n = 5$, bandwidth = 5%, ripple = 0.1 dB. (*Continued on next page*)

sidered to be caused by convergence errors in computation and by the fact that the sidewalls in the experiments are positioned farther than in the computation.

VI. Conclusions

The microstrip open end in a parallel-coupled stripline configuration has been characterized in a rigorous manner by a method based on a two-port resonance technique and full-wave field analysis. The analysis has shown that calculation results agree with those for isolated stripline open end in the asymptotic values as a large gap. The method has been confirmed by the experiments. Those calculated results were used for the design of experimental filters. The experimental results showed excellent filter performance which followed accurate design parameters. Thus, the method with the presented current basis functions will ensure accurate characterization in practice.

Appendix

For convenience in the formulation, Fourier integration is taken between $[-2a,2a]$ and $[-2b,2b]$; i.e., the Fourier transform $\tilde{\Phi}$ for Φ is defined as

$$\tilde{\Phi}(\alpha,\beta) = \int_{-2b}^{2b}\int_{-2a}^{2a} \Phi(x,z)e^{j(\alpha x+\beta z)}dx\,dz$$

$$\alpha = \frac{n\pi}{2a}, \qquad n = 0, \pm 1, \pm 2, \cdots$$

$$\beta = \frac{m\pi}{2b}, \qquad m = 0, \pm 1, \pm 2, \cdots.$$

The integrals of the currents accounting for both the real currents and fields and the image components due to the

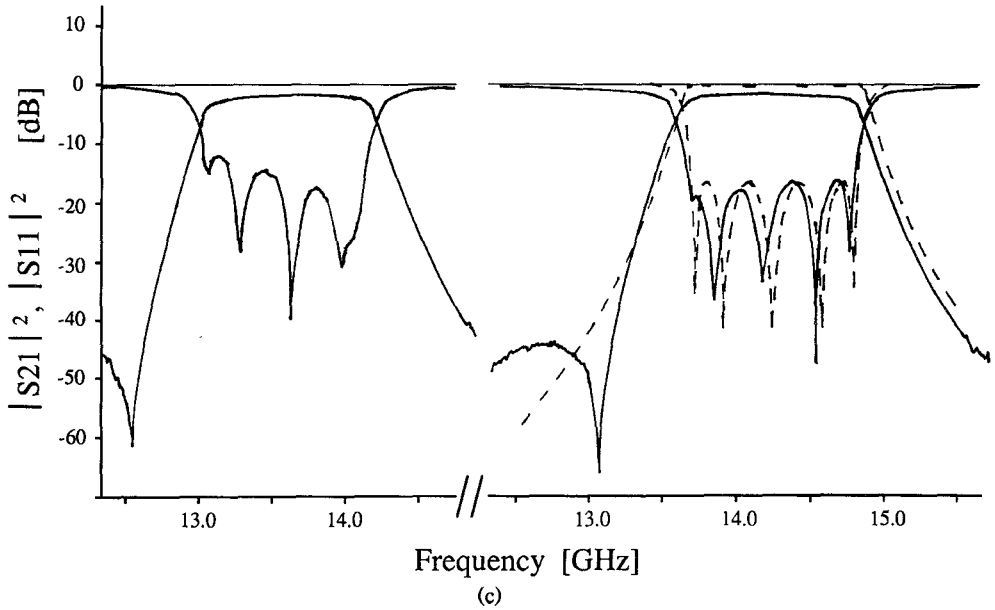

Fig. 7. (*Continued*). (c) $n = 5$, bandwidth = 8%, ripple = 0.1 dB (the same parameters as in Table I).

electric walls at the sidewalls lead to the following equations:

$$\tilde{J}z_{\mu}(\alpha,\beta) = \tilde{J}z_r^A(\beta)\tilde{J}z_s^A(\alpha) + \tilde{J}z_r^B(\beta)\tilde{J}z_s^B(\alpha)$$

$$= \begin{cases} j\dfrac{w\pi}{2}\{J_0(P)+J_0(Q)\}\left\{\dfrac{1}{A}\sin Al_h + \dfrac{1}{B}\sin \beta l_h\right\}\{\sin(\alpha d-\beta b)+(-1)^n\sin(\alpha d+\beta b)\}, & s=0,2,\cdots \\ j\dfrac{w\pi}{2}\{J_0(P)-J_0(Q)\}\left\{\dfrac{1}{A}\sin Al_h + \dfrac{1}{B}\sin Bl_h\right\}\{\cos(\alpha d-\beta b)+(-1)^n\cos(\alpha d+\beta b)\}, & s=1,3,\cdots \end{cases}$$

$$\tilde{J}x_{\mu}(\alpha,\beta) = \tilde{J}x_r^A(\beta)\tilde{J}x_s^A(\alpha) + \tilde{J}x_r^B(\beta)\tilde{J}x_s^B(\alpha)$$

$$= \begin{cases} j\dfrac{w\pi}{2}\{J_0(P)+J_0(Q)\}\left\{\dfrac{1}{A}\sin Al_h - \dfrac{1}{B}\sin Bl_h\right\}\{\cos(\alpha d-\beta b)+(-1)^n\cos(\alpha d+\beta b)\}, & s=1,3,\cdots \\ j\dfrac{w\pi}{2}\{J_0(P)-J_0(Q)\}\left\{\dfrac{1}{A}\sin Al_h - \dfrac{1}{B}\sin Bl_h\right\}\{\sin(\alpha d-\beta b)+(-1)^n\sin(\alpha d+\beta b)\}, & s=2,4,\cdots \end{cases}$$

where

$$A = \frac{2r-1}{2l_h}\pi - \beta \qquad P = \frac{w}{2}\left(\alpha + \frac{s\pi}{w}\right)$$

$$B = \frac{2r-1}{2l_h}\pi + \beta \qquad Q = \frac{w}{2}\left(\alpha - \frac{s\pi}{w}\right)$$

$$l_h = L + b$$

with J_0 the zero-order Bessel function of the first kind.

Acknowledgment

The author wishes to thank Dr. Y. Nagakoka, Director of the Image Technology Research Laboratory, for providing the opportunity to carry out this work. The author would also like to thank H. Ikeda and Y. Tsujimoto for their expert assistance in the experiments.

References

[1] S. B. Cohn, "Parallel-coupled transmission-line-resonator filters," *IRE Trans. Microwave Theory Tech.*, vol. MTT-6, pp. 223–231, Apr. 1958.

[2] Y. Konishi and Y. Utsumi, "Parallel coupled microstrip bandpass filter with arbitrary angle," *IECE Trans.*, vol. 57-B, no. 7, pp. 467–469, July 1974 (in Japanese).

[3] P. B. Katehi and L. P. Dunleavy, "Microstrip filter design including dispersion effects and radiation losses," in *IEEE MTT-S Int. Microwave Symp. Dig.*, June 1986, pp. 687–690.

[4] J. Zehentner, "Analysis and synthesis of coupled microstrip lines by polynomials," *Microwave J.*, pp. 95–98, May 1980.

[5] R. H. Jansen, "Hybrid mode analysis of end effects of planar microwave and millimetre wave transmission lines," *Proc. Inst. Elec. Eng.*, vol. 128, pt. H, no. 2, Apr. 1981.

[6] EMSim(Moment method), EEsof, Westlake Village, CA 91362; also LINMIC+(SDA), Compact Software Inc. Paterson, NJ 07504.

[7] W. Y. Lau, "Network analysis verifies models in CAD packages," *Microwaves and RF*, pp. 99–110, Nov. 1989.

[8] R. Sorrentino and T. Itoh, "Transverse resonance analysis of finline discontinuities," *IEEE Trans. Microwave Theory Tech.*, vol. MTT-32, pp. 1633–1638, Dec. 1984.

[9] T. Itoh, "Analysis of microstrip resonators," *IEEE Trans. Microwave Theory Tech.*, vol. MTT-22, pp. 946–952, Nov. 1974.

[10] T. Itoh, *Numerical Techniques for Microwave and Millimeter-Wave Passive Structures*. New York: Wiley-Interscience, 1989, ch. 5.

[11] T. Uwano, "Accurate characterization of microstrip resonator open end with new current expression in spectral-domain approach," *IEEE Trans. Microwave Theory Tech.*, vol. 37, pp. 630–633, Mar. 1989.

[12] R. A. Dell-Imagine, "A parallel coupled microstrip filter design procedure," in *IEEE G-MTT Int. Microwave Symp. Dig.*, 1972, pp. 29–32.